

# THE HIGH SEISMIC PERFORMANCE CONCEPT OF INTEGRATED BRIDGE PIER WITH TRIPLE RC COLUMN ACCOMPANIED BY FRICTION DAMPER PLUS GAP

S. ANGGA FAJAR<sup>1</sup> and Y. TAKAHASHI<sup>2</sup>.

<sup>1</sup>Phd. Student, Dept. of Urban Management, Kyoto University  
(C1 Bldg. R. 146, Katsura Campus, Kyoto 615-8245, Japan)  
E-mail: [angga.setiawan.85z@st.kyoto-u.ac.jp](mailto:angga.setiawan.85z@st.kyoto-u.ac.jp)

<sup>2</sup>Member of JSCE, Professor, Dept. of Civil and Earth Resource Eng., Kyoto University  
(C1 Bldg. R. 455, Katsura Campus, Kyoto 615-8245, Japan)  
E-mail: [takahashi.yoshikazu.4v@kyoto-u.ac.jp](mailto:takahashi.yoshikazu.4v@kyoto-u.ac.jp)

The structural performance concept of the bridge in Japan considers two levels of seismic performance which realizes elastic behavior under common earthquake then prevents the structure collapse and limits the structure damage under severe earthquake. Also, the behavior and the parameter of reinforced concrete (RC) column accompanied with friction device were determined successfully based on the experiment and numerical analysis. On the other hand, the problem of medium span bridge bearing support in the regions where to have extreme temperatures fluctuation is deterioration. It is triggered by the superstructure suppression which sustains thermal expansion, creeps, and shrinkages phenomena. This study proposes the structural system of integrated bridge pier with triple RC column accompanied by friction damper plus gap which substitutes the conventional bridge pier structural system. Numerical analysis is performed for this system with fiber element model. It shows that the proposed structure has an excellent performance not only under small deformation to allocate thermal expansion of the superstructure but also under seismic load. The structural simulations with different limit state of column location and the different yield strength of reinforcing steel configuration are conducted to get better structural cost-performance option.

**Key Words :** *steel pipes, shear panel damper, dissipated energy, high seismic performance, deformation limit*

## 1. INTRODUCTION

The seismic design concept of the bridge in Japan is that the structure must be secure in seismic performance. The structure is intended to localize the damage limit and prevent collapse at large earthquake loads. During the service period, small earthquakes are likely to occur so that the structure must be able to behave elastically. At the lifetime design, large earthquakes are unusually to occur, structures are permitted to have plastic behavior, but structural damage is limited<sup>6)</sup>.

The previous researcher below proposed some kinds of passive energy dissipated for seismic control of structure which implement friction device. A

large cantilever panel structure connected with limited slip bolt joints for seismic control of building was developed by Pall<sup>14)</sup>. Also, the concept of the friction damped braced frame of steel structure was proposed by Pall and Marsh<sup>16)</sup>. Mualla and Belev<sup>9)</sup> Mualla and Belev [11] developed rotated friction damping device (FDD) with a V-bracing shape for seismic control of steel structure.

The experiments of high seismic performance column under cyclic loading have been performed by Nakamura et al.<sup>11)</sup>. This structure consists of three parts of thin concrete columns linked to friction devices with prestressed bolts shown in **Fig. 1**. Based on the experimental results, this structure has a considerable deformation capacity elasticity with

high energy dissipation. The elastic deformation capacity of the structure is about 2.0% of drift ratio. Also, it has a fairly constant resistance up to a 10% of drift ratio<sup>10)</sup>. According to FEMA 356<sup>2)</sup>, in the performance of Immediate Occupancy, the limitation of the main reinforced concrete column structure is small hairline cracks, the possibility of limited plasticization in some locations and no damage to the 1.0% drift ratio under temporary conditions and no permanent drift. This structure type is expected to correspond to important or dangerous facility categories that achieve Immediate Occupancy performance under severe earthquakes with small probability of occurrence.

The reinforced concrete column accompanied by this friction damper has high potential to be implemented on the bridge pier structure. With elastic deformation capacity and sufficient energy dissipation, this structure is capable of behaving elastically at Level 2 of seismic design based on JRA standard<sup>6)</sup>.

On the other hand, there is a problem with the support of bridge structures with short to medium spans in Japan i.e. deterioration occurs before the seismic load design works on the structure, as shown in Fig. 2a. This is triggered by the longitudinal displacement load caused by the expansion of the upper structure bridge due to the phenomenon of thermal expansion, crawl, and shrinkage.

The objective of this research is to develop modified reinforced concrete columns accompanied by frictional damper. This structural system is expected to replace conventional bridge pier consisting of column and bearing support. The expectation

is that this structure can be implemented for future generation of the short-medium span bridges by removing bearing support, as shown in Fig. 3. The friction damper plus gap (FDG) is expected to realize high flexibility in small deformations. When the seismic load design occurs, the friction damper works to absorb the vibrational energy under the condition of the structure still below its limit state of performance target. The application of reinforcing steel materials and the location of different limit states is expected to consider regarding cost and structural performance relationship. The expected performance target is the structure behaving elastically (called Performance I) under severe earthquake excitation (called Level 2). Numerical analysis with nonlinear static and dynamic is performed to simulate this proposed structure by implementing the fiber-frame elements model.

## 2. RC COLUMN ACCOMPANIED BY FRICTION DAMPER PLUS GAP

### (1) Friction damper

Pall et al.<sup>15)</sup>, Mualla and Belev<sup>9)</sup> and Moralez et al.<sup>17)</sup> implement the elastoplastic idealization of friction damper in the numerical analysis based on experimental results. The friction device follows the Coulomb rule of with dry friction law, the frictional force in both conditions of sticky and slip is assumed to be constant. The friction coefficient ( $\mu$ ) is the friction force ratio ( $F_{max}$ ) with normal force ( $N$ ) which can be determined as:

$$\mu = \frac{F_{max}}{N} \quad (1)$$

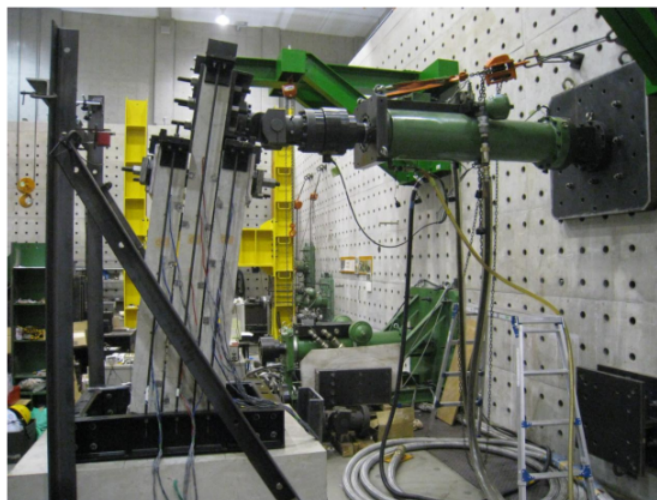


Fig. 1 The experiment of RC column accompanied by friction damper<sup>10)</sup>



(a)



(b)

**Fig. 2** The deterioration of bridge bearing support; (a) rubber bearing type and (b) pin bearing type

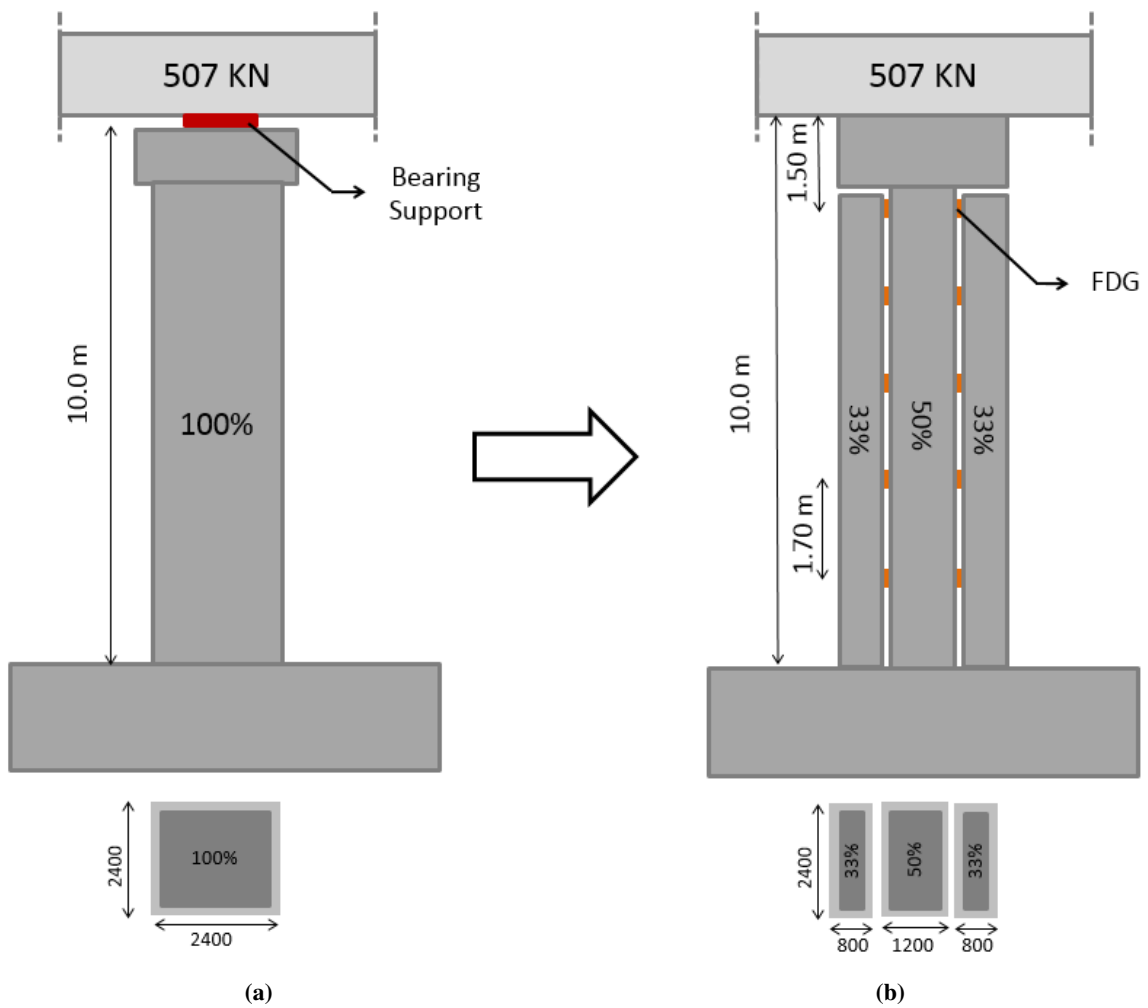


**Fig. 3** (a) The conventional bridge pier and (b) the proposed bridge pier accompanied by FDG.

Mualla and Belev<sup>9)</sup> have conducted experiments and numerical analysis of steel portal structures with friction damper devices (FDD) containing friction material (free friction asbestos material plus high-performance steel materials). The cyclic load test is 400 cycles; the result is almost no damage to FDD.

Nakamura et al.<sup>12)</sup> conducted a friction device testing experiment consisting of SS400 steel type friction material paired with SUS304 steel type material. The experiment results show that along with the increase in the slip the coefficient value of friction increases close to linear, starting from about 0.2 at the beginning of slip occurs reaching about 0.5 at

**Table 1** The variable of structural parameters.

Str. Name	Scenario	Gap (mm)	Reinforcing steel yield strength (Mpa)		yield lim. loc.
			Middle Column (MC)	Side Column (SC)	
Str1	1	0.00	345	345	MC
Str2	1	10.00	345	345	MC
Str3	1	20.00	345	345	MC
Str4	1	30.00	345	345	MC
Str5	1	w/o FD	345	345	MC
Str6	1	Rigid FD	345	345	MC
Str7	2	0.00	685	345	MC
Str8	2	10.00	685	345	MC
Str9	2	20.00	685	345	MC
Str10	2	30.00	685	345	MC
Str11	2	w/o FD	685	345	MC
Str12	2	Rigid FD	685	345	MC
Str13	3	0.00	685	685	MC
Str14	3	10.00	685	685	MC
Str15	3	20.00	685	685	MC
Str16	3	30.00	685	685	MC
Str17	3	w/o FD	685	685	MC
Str18	3	Rigid FD	685	685	MC
Str19	4	0.00	685	685	SC
Str20	4	10.00	685	685	SC
Str21	4	20.00	685	685	SC
Str22	4	30.00	685	685	SC
Str23	4	w/o FD	685	685	SC
Str24	4	Rigid FD	685	685	SC
Str25	-	Conv. RC	345	-	-
Str26	-	Conv. RC	685	-	-

**Table 2** The variable of the FDG confinement force.

Variable no.	Maximum confinement (KN)	con- force
1	0	
2 to 41	4200-12000	incr. 200
42	very large	

**Table 3** The reinforcing steel parameter input.

$f_y$ (MPa)	$E$ (MPa)	$b$	$R_0$	$c_{R1}$	$c_{R2}$
345	200000	0.02	19.5	0.925	0.5
685	200000	0.02	19.5	0.925	0.5

the end of loading.

## (2) The structural concept of RC pier accompanied by FDG

The principle of the column accompanied by the FDG is that the structure still behaves elastically in small deformation conditions due to an expansion

of the bridge structure as well as to large deformations due to seismic loads with sufficient energy dissipation. To achieve a large elastic deformation capacity, the column structure is composed of three thin columns. The friction device unifies each component of the column through the bolts prestressed in the lateral direction. The energy of dissipation

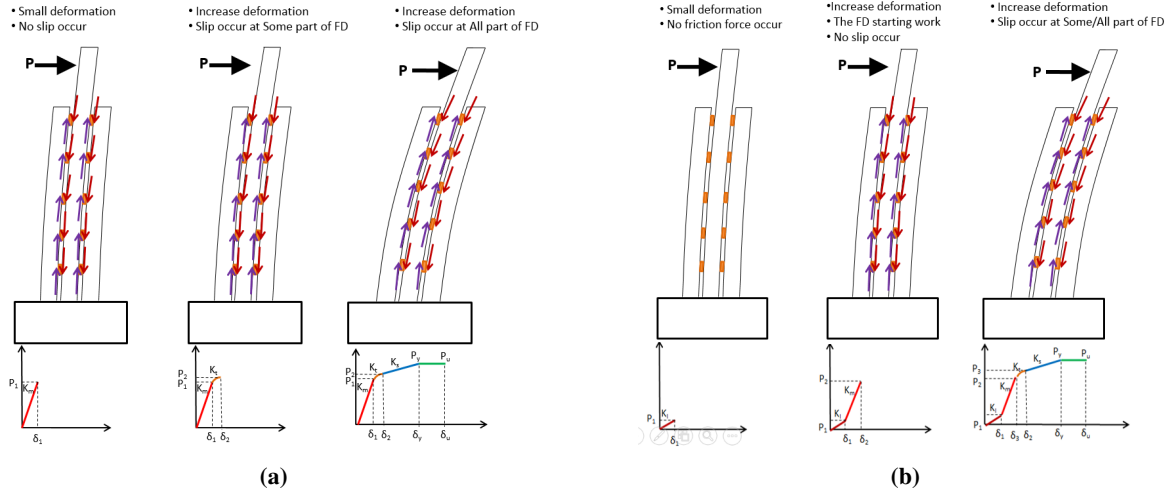


**Fig. 4** The mechanism of RC columns accompanied by friction damper; (a) without gap<sup>10)</sup> and (b) with gap.

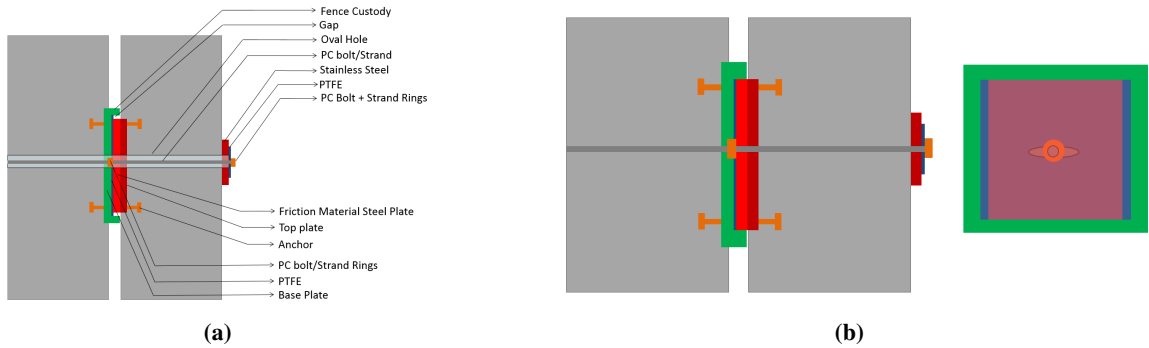


**Fig. 5** The component of proposed FDG; (a) side view and (b) top view.

is produced by the slip deformation of the friction device due to the lateral deformation of the structure<sup>10)</sup>.

The structure friction damper without the gap has four stages of stiffness. When small lateral loads ( $P$ ) work to the top of the column, minor lateral deformations occur, slippage has not occurred in the friction damper. At this stage, the stiffness of the column is the stiffness of the monolith ( $K_m$ ). On the other hand, the larger lateral force ( $P$ ) induces greater deformation of the column; the slip occurs in some portion of the friction damper, the column stiffness decreases to the transition stiffness ( $K_t$ ). Increased column lateral deformation will induce all friction damper to slip so that separate stiffness ( $K_s$ ) is formed. Separate stiffness is expected to occur in elastic fixed structural conditions before longitudinal steel reinforcements are yielding. After the yielding of the longitudinal steel reinforcement, the stiffness continues to experience plastic stiffness ( $K_p$ ). The illustration of the stiffness stage of the structure is shown in **Fig. 4a**. When comparing the four different structural systems as shown in

**Fig. 6b**, the column structure behaves in a monolithic manner having greater stiffness and strength than the separate parts, whereas the part that the group structure of the columns behaves separately has a greater elastic deformation capacity.

The columns accompanied by FDG have the same initial stiffness as the group of columns behaving separately, while the ultimate strength approaches the monolithic group of columns behaving. The elastic deformation capacity looks like a structure that has separate stiffness as shown in **Fig. 4b** and **Fig. 6b**.

### (3) The characteristic of friction damper plus gap

To accommodate slipping and bearing action at the gap margin, FDG is composed of a slip surface connected to a base plate with a slit retaining and steel plate with PTFE surface. To produce friction of the friction surface connected by a top plate with a SUS304 steel type paired with a steel plate with SS400, the illustration can be seen in **Fig. 5**. In the numerical model, the FDG is expected to have me-

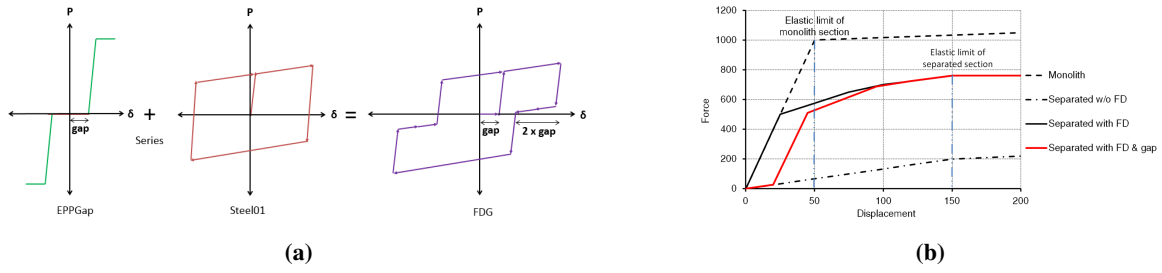


**Fig. 6** (a) The material idealization of FDG in the numerical model and (b) the comparison of structural behavior in the global response.

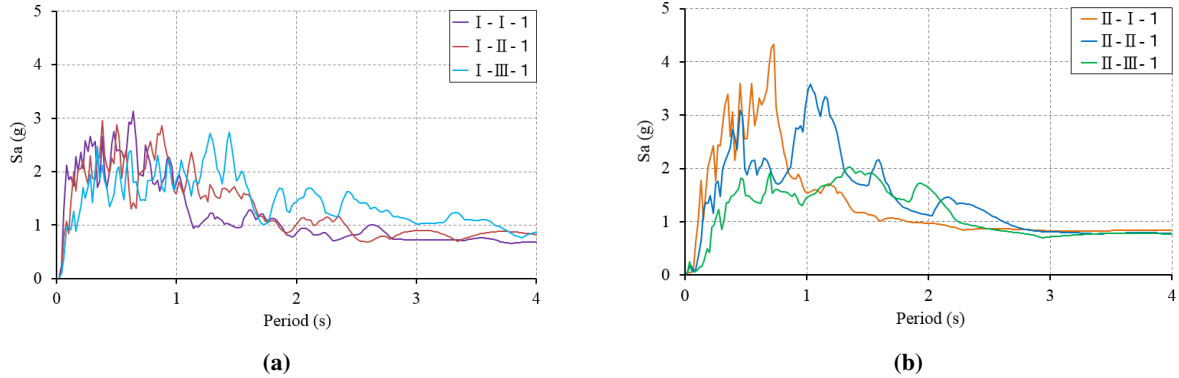


**Fig. 7** The response spectra of Level 2 Type II seismic design<sup>6)</sup>; (a) Type I and (b) Type II.

chanical behavior with a combination of series of Elastic Perfect Plastic Gap (EPPGap) and bilinear (Steel01) material models as shown in **Fig. 6a**.

#### (4) The proposed bridge pier structure with FDG

A gap in the FDG causes the group of columns to deform in a separate behavior over the length of the gap so that the initial stiffness is equal to the stiffness of the separate-section columns. When the deformation of the structure has exceeded the length of the gap, the structure will behave as a monolith part, the illustration of the mechanism can be seen in **Fig. 4b**.

The seismic performance target of this structure is the seismic response of the structure still below its limit state at Level 2 of earthquake. The limit state on this proposed structure is to embody structures that behave closely to the elastic state characterized by a sufficiently large post-yield stiffness. This determination is aimed at preventing residual deformation and structural damage during and after the earthquake as an effort to reduce consumption of recovery and restoration times.

There are four limiting scenarios as shown in **Ta-**

**ble 1** which the reinforcing steel grade in the middle and side columns is made in different structural configurations. Strict state limits (full elastic conditions) are proposed by the elastic restriction on the edge column. While the loser (semi-elastic) limit state is proposed by elastic limits in the middle of the column section, which means that reinforcing steel in the side part of column occur yield, but the middle column has not yielded. The purpose of using structural configurations with different reinforced steel material grades (SD345 and USD685) is to provide a choice of structural material requirements that are consequently cost-effective to the seismic performance of the structure.

### 3. METHODOLOGY

In this study, there are four scenarios of the proposed numerical model structure with each of the six variations to determine the behavior and performance of the structure. This scenario is a combination of the application of steel material quality and the location of the state limit review of the structure as shown in **Table 1**.

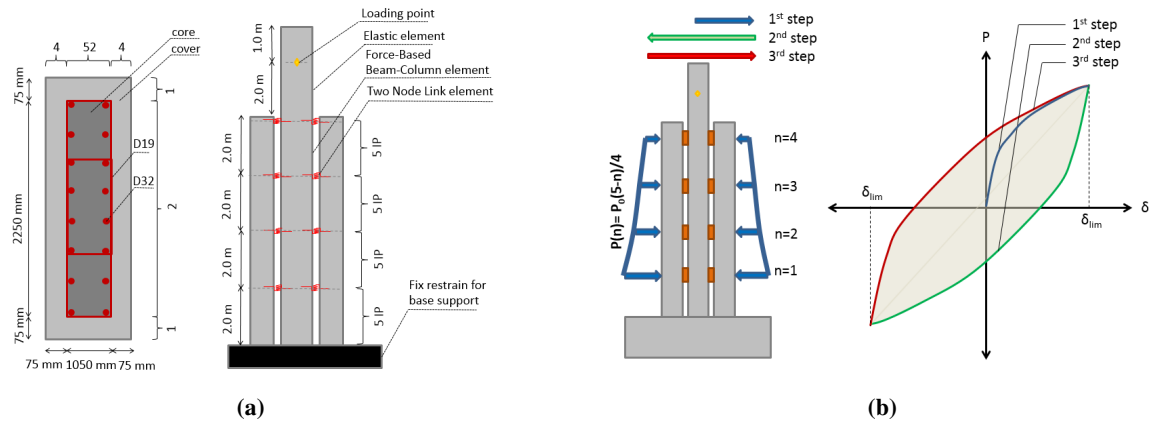


**Fig. 8** The structural idealization in the numerical model and (b) the confinement force distribution and the dissipated energy calculation method of the structure.

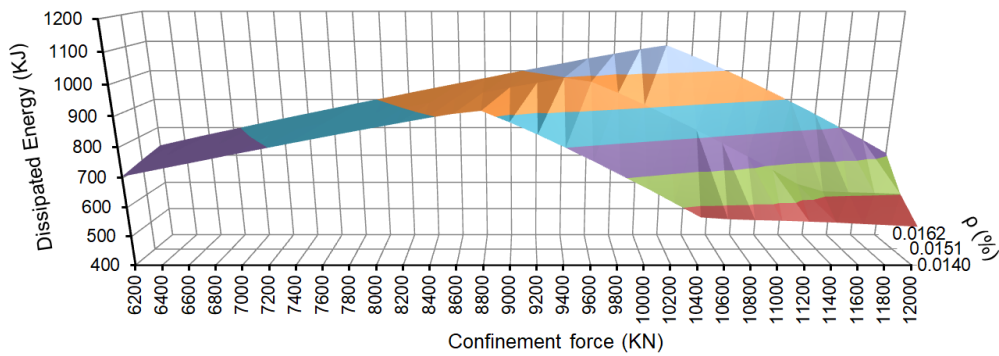


**Fig. 9** The dissipated energy influenced by the FDG confinement force and the proportion of reinforcing steel.

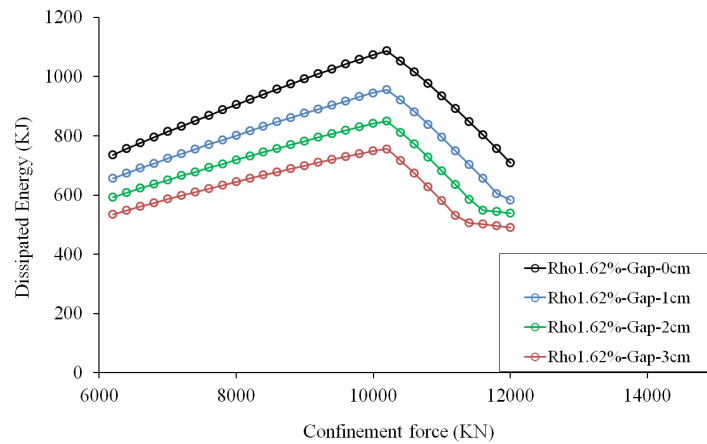


**Fig. 10** The dissipated energy influenced by the gap length.

### (1) The structural behavior investigation methods

The structural behavior that needs to be observed and investigated is the structural rigidity at the small deformation (accommodating the deformation of upper structural expansion), the deformation limit capacity, and also the quantity of energy dissipation of the structure. Static pushover analysis in each gap length variation (10 mm, 20 mm, and 30 mm) was performed including structural stiffness observation and comparison without the use of a gap (0

mm of gap). The effectiveness of gaps implementation in reducing the initial stiffness of the structure can be evaluated.

Structures that have large deformation limit capacities are expected structures because in addition to the resulting energy dissipation capacity will be larger; such structures will have behavior that is closer to the elastic conditions in large earthquake excitations. The dissipated energy is also an important parameter of structural behavior because it involves the significance of structures in dampen-

ing seismic excitation. The existence of the gap will certainly reduce the energy dissipation, then the determination of the length should pay attention to the impact of energy dissipation reduction. In this

study, the ratio of the gap length effect to the dissipated energy generated by the structure is also carried out.

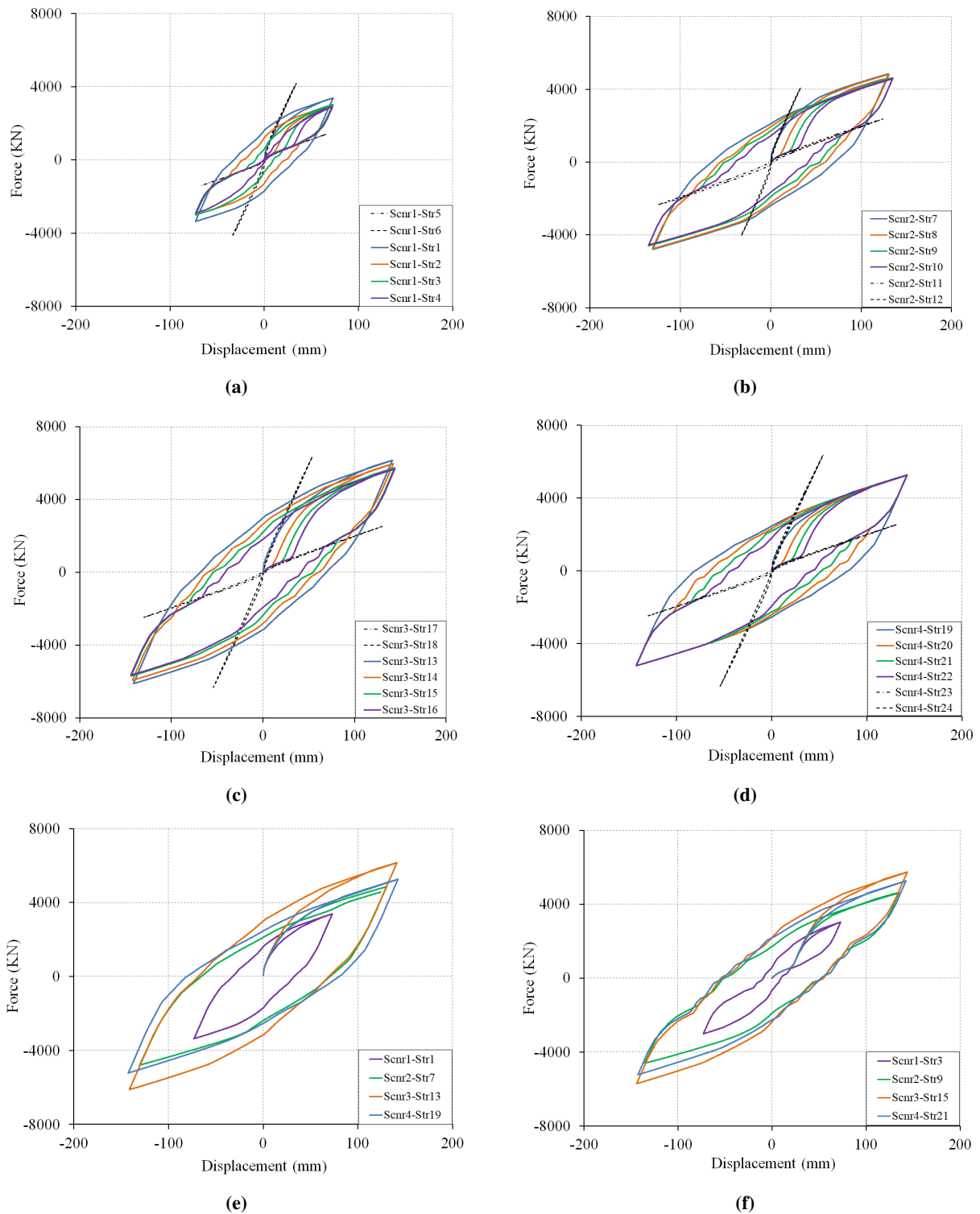


**Fig. 11** The hysteresis curve comparisons under static cyclic analysis; (a) Scenario1, (b) Scenario2, (c) Scenario3, (d) Scenario4, (e) structure without gap, and (f) structure with 20 mm gap.

## (2) The structural performance investigation methods

To examine structural performance, the structure is simulated by full-scale numerical analysis. This study refers to the reference design of Iemura, Takahashi, and Sagobe<sup>5</sup> i.e. conventional reinforced concrete structures designed under JRA code<sup>6</sup> applied as a benchmark of the proposed structure. The bridge pier has a height of 9.6 m, supporting 507 tons of structural mass over the bridge with a ductility value of 5. The column has a 2.4x2.4 m<sup>2</sup> section with longitudinal reinforcement of 1.20% of the concrete cross section (72D35, 345 MPa) and it is assumed that the concrete has a compressive strength of 37 MPa. The transversal reinforcing steel consist of 4D19 with a distance of 150 mm. The conventional RC pier is simulated to make structural performance comparisons. There are two types of conventional structures, developing reference<sup>5</sup> structures varied again with different steel reinforcing classes, namely SD345 and USD685.

The performance of the proposed structure was compared with conventional reinforced concrete pillars which were modified to 10.0 m in height by 1.40%, 1.51%, and 1.62% of the reinforcement range with 0 mm, 10 mm, 20 mm, and 30 mm in 42 variations of friction damper confinement force are shown in **Table 1**. The reinforced concrete column section with FDG is designed with a total area of 116% of the conventional pillar with a 33%-

50%-33% configuration as shown in **Fig. 3**. The structural configuration is determined with an area greater than 100% of the structure in reference<sup>5</sup> because in theory, its strength is smaller than the monolith column structure illustrated as in **Fig. 6b**.

In this study, structural parameters that are estimated to have significant influence include the force of restriction on the friction device, the area needs longitudinal steel reinforcement and the length of the gap. The structure is assumed to be capable of accommodating deformation due to thermal expansion up to 20 mm (bridge span 40 m,  $\Delta t = 40^\circ \text{C}$ ,  $\alpha = 1.2e-5 \text{ m/m}^\circ \text{C}$ ). In this case, the confinement distribution pattern is implemented along the height of the pier as shown in **Fig. 8b**. The behavior of the largest energy dissipation structure and capacity in the FDG confinement force variable was selected and verified its seismic performance.

Nonlinear analysis includes static pushover and dynamic time history performed to observe the structural behavior in each deformation limit and maximum large structural response (called Level 2). Verification of seismic performance of the structure is conducted by applying a Level 2 earthquake excitation with Type I and Type II, each of which consists of three different excitation types of ground. Response spectra of the earthquake excitation inputs are respectively presented in **Fig. 7**. Also, the residual deformations of the structure after the earthquake excitation are examined to confirm the recentering capability.

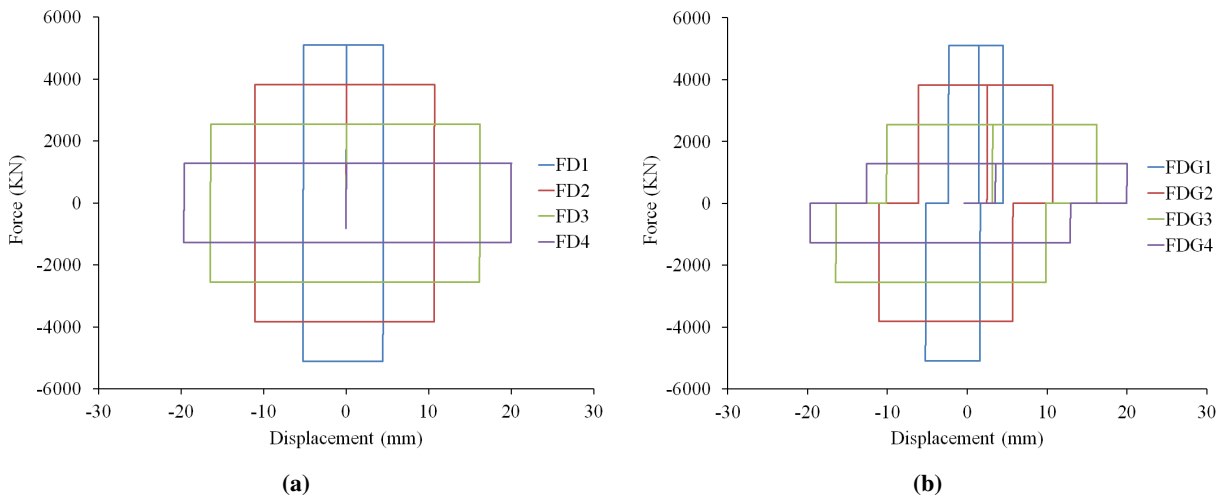


**Fig. 12** The SPD hysteresis curves of; (a) Str19 and (b) Str21.

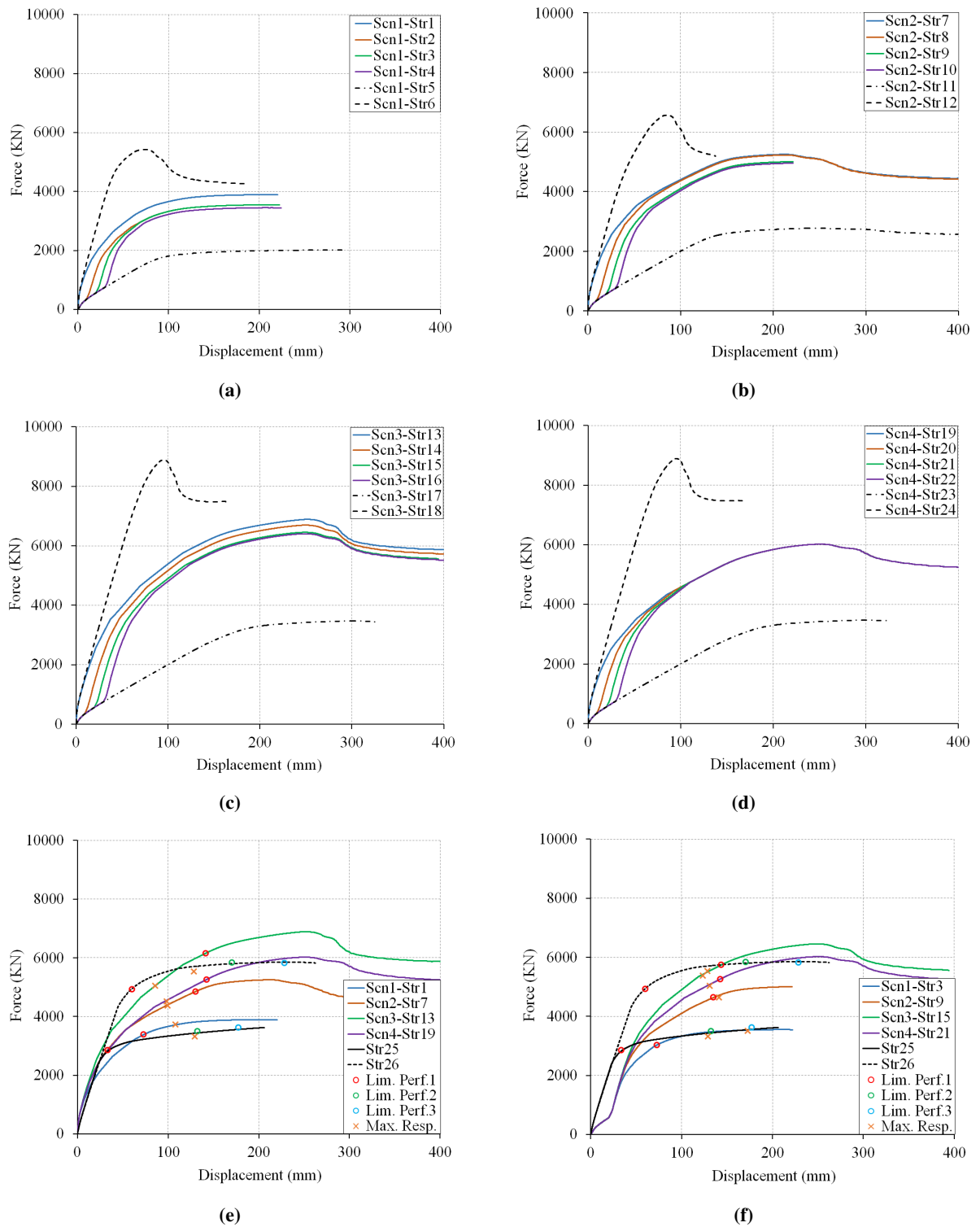


**Fig. 13** The skeleton curve under static pushover analysis; (a) Scenario1, (b) Scenario2, (c) Scenario3, (d) Scenario4, (e) structure without gap, and (f) structure with 20 mm gap.

## 4. NUMERICAL ANALYSIS

### (1) Structural idealizations

The reinforced concrete columns coupled with FDG to be idealized as frame elements in a two-dimensional model with three degrees of freedom. The right type of element needs to be considered

based on the specimen mounting conditions. The upper end of the center column is idealized as an elastic element to simulate the support of the loading point which should have elastic behavior with the provision of a steel jacket structure system. For dynamic analysis, centralized one-point mass idealization is expected to achieve the ease of numerical

convergence. The upper structure masses of bridges and piers are placed at 10.0 m height.

The implementation of Force-based Beam-column element with a fiber cross section applied to the main column element<sup>4,21,20,13,18</sup>. The number of sufficient integration points of the frame element and the number of fibers in the column cross section should be determined to obtain a convergent and accurate result. The concrete materials and steel materials used for the reinforced concrete column columns are respectively Concrete02 and Steel02 with the properties as shown in **Table 3**. The idealization of the structure model is illustrated as in **Fig. 8a**.

The friction device is idealized as a Two-node link element that is coupled in series with Steel01 and EPPGap material in a high alignment direction of the piers and the elastic material is applied in the direction of the column perpendicular high as the embodiment of the PC bar behavior. The FDG material parameters will be discussed in the sub-section of the FDG material parameters below.

### (2) Steel and concrete material parameters

The reinforcing steel materials modeling applies Steel02 based on Giuffre-Menegotto-Pinto theory<sup>8</sup>). The reinforcing steel material input parameters include;  $f_y$  is the power of melting,  $E$  is the modulus of elasticity,  $b$  is the hardening ratio and the parameters for controlling the transition between the elastic branches to the plastic branches are  $R_0$ ,  $c_{R1}$  and  $c_{R2}$ . The reinforced steel material parameters are selected following the recommendations of reference<sup>3</sup>) as shown in **Table 2**. While the column elemental concrete material is modeled as a Concrete02 material based on the reference<sup>7</sup>) to a material constituted by reference<sup>6</sup>). In this study, concrete quality is assumed to be C30 ( $f_c = 30$  MPa).

### (3) Friction damper plus gap parameters

The friction material is idealized as a bilinear material model, the elastic condition describing the sticky state, whereas the post-yielding state indicates that the slip state has occurred. Friction damper materials are idealized as Steel01 material that can behave isotropic and kinematic hardening based on Fedeeas<sup>1</sup>. In this study, the behavior of cyclic hardening of FDG materials was idealized as kinematic hardening.

The value of the friction coefficient is assumed to be 0.5 with the hardening ratio close to zero and the slip deformation is 0.025 mm. Friction device parameters were achieved as a result of some numer-

ical analysis experiments from previous studies<sup>19</sup>). Based on several pilot analyzes, the friction coefficient and slip deformation are the most important parameters that play an important role in the formation of hysteretic curves and the distribution of curvatures along the column heights<sup>19</sup>).

The frictional component of FDG resulting from a combination of Elastic Perfect Plastic Gap (EPP-Gap) material series and Steel01 material as in **Fig. 6a**. EPPGap material works to simulate slip action across the gap. At the end position of the gap length, the stiffness and the strength of the EPP-Gap material are defined sharply greater than the steel material parameters (Steel01) on the friction device to reflect the slip deformation determined by the dominant friction surface.

### (4) Numerical analysis scenarios

The numerical analysis consists of three stages: static cyclic analysis, static pushover analysis and dynamic analysis with earthquake excitation. The static cyclic analysis is implemented to investigate structural behavior including force and deformation relationships as well as the energy capacity of dissipation on structural deformation limit. Static pushover analysis to determine the shape of the skeleton curve to the ultimate structural deformation condition. While the dynamic analysis to find out the structure response and to verify the performance of the structure under Level 2 of the seismic design.

In the cyclic loading analysis, there are two stages of the loading pattern, the first is the equivalent gravitational load in the form of a constant nodal load pattern and the second is a cyclic load in the form of a linearly displaced load on the node. A cyclic load investigating the boundary of the elastic state and calculating the energy of dissipation is assumed to be a moving load of 3 steps to the center of the mass of the structure at a height of 10.0 m as shown in **Fig. 8b**. Equivalent gravity loads apply load control integrators to Newton's algorithm, whereas cyclic load implements integrator displacement control with the Newton algorithm<sup>7</sup>). Equivalent gravity loads to be applied directly without increment, otherwise, the dynamic excitation load implements a time interval of 0.001 s.

To examine the recentering capability of the structure, the residual deformations after earthquake are recorded in the state before and after the confinement force of FDG to be released. The deformation of the structure after the earthquake loading time history is also recorded for 5 seconds. During

**Table 4** The stiffness comparison at the small deformation.

Disp. (mm)	The structural stiffness with the gap length ( $K_{ef}$ , KN/m)				The structural stiffness ratio with the gap length (ratio $K_{ef}$ )			
	0 mm	10 mm	20 mm	30 mm	0 mm	10 mm	20 mm	30 mm
0.10	434083.47	45254.56	45254.56	45254.56	1.00	0.10	0.10	0.10
10.00	147214.38	38426.31	35829.41	35829.41	1.00	0.26	0.24	0.24
20.00	110595.51	69624.47	28570.04	28387.38	1.00	0.63	0.26	0.26
30.00	90735.87	76979.29	51619.02	25611.03	1.00	0.85	0.57	0.28

**Table 5** The seismic performance of the structures.

Str. Name	Max. conf. force (KN)	Total dissipated energy	Percentage dissipated energy of FDG	Equal energy damping	Deformation response of earthquake			Residual deformation		
					Max.	Ratio	Eq. no.	Before released	After released	Eq. no.
Str1	7400	332.73	0.96	0.21	107.87	1.48	II-I-1	10.68	9.21	II-I-1
Str2	6000	232.79	0.98	0.17	156.49	2.15	II-III-1	19.50	15.75	II-III-1
Str3	6000	171.11	0.97	0.12	172.69	2.37	II-II-1	27.65	24.23	II-III-1
Str4	5600	117.30	0.96	0.09	208.52	2.87	II-II-1	18.90	18.92	II-I-1
Str5	0	2.27	0.00	0.00	260.59	3.93	I-II-1	22.24	22.21	I-II-1
Str6	~	9.13	0.00	0.01	64.53	1.89	II-II-1	6.13	6.99	II-I-1
Str7	10400	875.33	0.65	0.22	99.46	0.76	II-I-1	8.49	6.16	II-I-1
Str8	10200	760.85	0.65	0.19	128.98	0.98	II-I-1	7.74	5.09	I-II-1
Str9	8800	709.36	0.83	0.18	141.59	1.05	II-III-1	7.00	3.18	I-II-1
Str10	8600	626.11	0.84	0.16	162.05	1.20	I-II-1	7.58	7.09	I-II-1
Str11	0	16.79	0.00	0.01	151.94	1.23	I-I-1	1.20	1.26	I-I-1
Str12	~	7.29	0.00	0.01	68.78	2.10	II-I-1	2.49	5.33	II-I-1
Str13	13800	1220.04	0.97	0.22	85.52	0.61	II-I-1	6.33	4.02	II-I-1
Str14	13000	1048.47	0.97	0.20	120.97	0.85	II-I-1	5.22	5.41	II-II-1
Str15	12000	918.56	0.97	0.18	123.44	0.86	II-III-1	4.23	3.04	II-III-1
Str16	11800	809.41	0.97	0.16	148.65	1.03	I-II-1	4.73	3.22	I-II-1
Str17	0	10.65	0.00	0.01	285.68	2.18	I-III-1	30.67	30.97	II-I-1
Str18	~	13.69	0.00	0.01	71.74	1.33	II-I-1	1.13	1.65	II-I-1
Str19	10200	1086.84	0.98	0.23	98.31	0.69	II-I-1	4.62	2.69	II-I-1
Str20	10200	955.50	0.98	0.20	126.76	0.89	II-I-1	5.58	4.44	II-II-1
Str21	10200	849.94	0.98	0.18	131.12	0.92	II-III-1	5.56	4.12	I-II-1
Str22	10200	755.77	0.97	0.16	153.82	1.08	I-II-1	6.57	4.16	I-II-1
Str23	0	10.65	0.00	0.01	285.68	2.18	I-III-1	30.67	30.97	II-I-1
Str24	~	13.69	0.00	0.01	71.74	1.33	II-I-1	1.13	1.65	II-I-1
Str25	-	-	-	-	129.13	3.85	II-I-1	15.01	-	II-III-1
Str26	-	-	-	-	128.36	2.14	II-I-1	11.41	-	I-II-1

the recording of that time, the average deformation of the structure is calculated. There are two types of post-earthquake structural deformation records namely; the FDG condition still merges with structure, and the FDG state has been removed from the structure (confinement force released after earthquake event). The recording of the two deformation

records is performed respectively at ( $T_{eq}$  to  $T_{eq}+5$ ) and ( $T_{eq}+15$  to  $T_{eq}+20$ ) when at the time ( $T_{eq}+15$ ), the FDG is released under free vibration. The objective of deformation observation with two different scenarios is to know the residual deformation and the ability of recentering the structure after the earthquake.

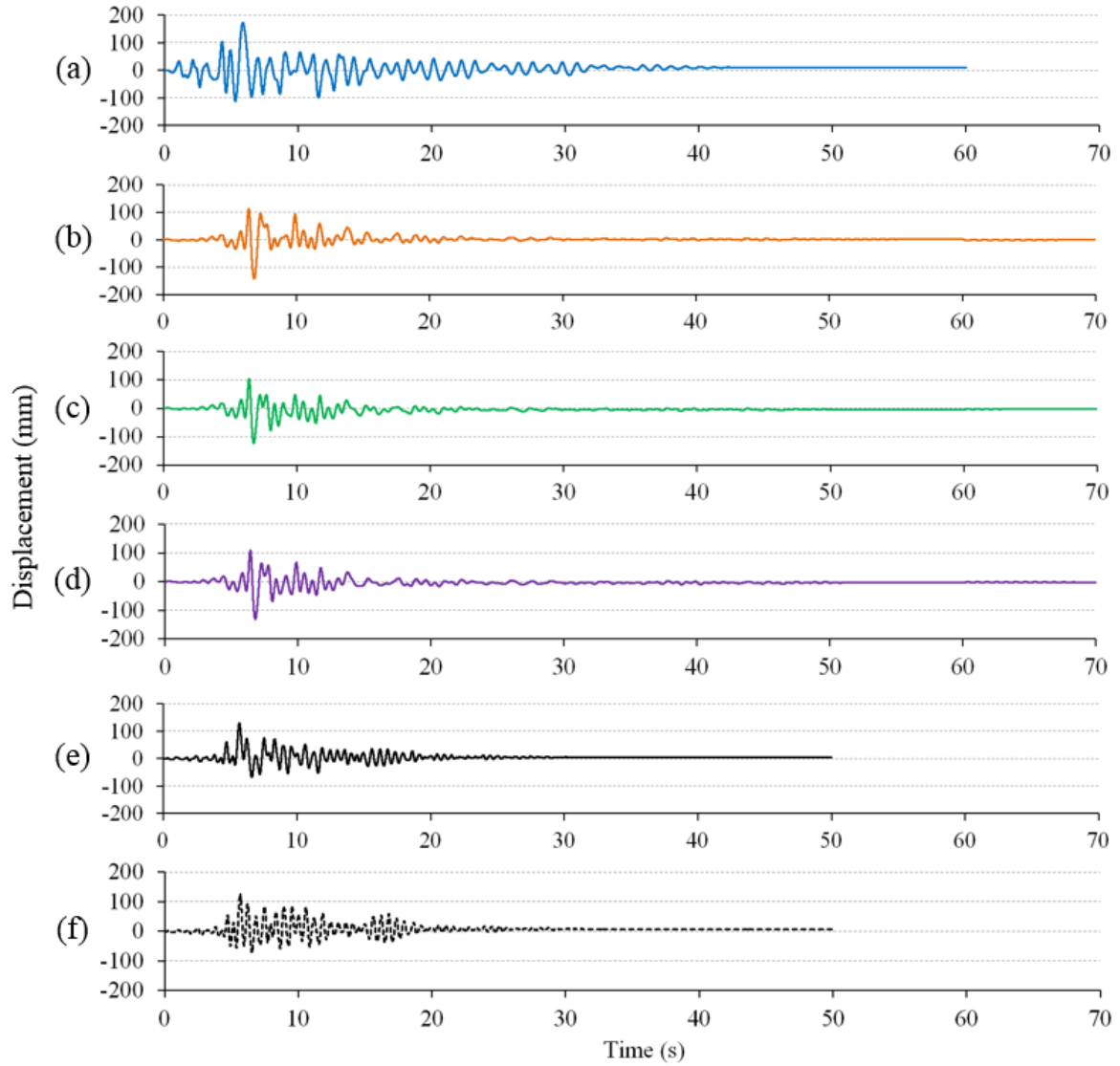


**Fig. 14** The maximum displacement response of the structure under seismic load level 2; (a) Str3, (b) Str9, (c) Str15, (d) Str21, (e) Str25, and (f) Str26.

## 5. RESULTS

### (1) Structural behavior

The stiffness ratio of the proposed structure with no gaps is shown in **Table 4**. The proposed structure has small initial stiffness and large elastic deformation limit capacity, thus having the ability to accommodate thermal deformation. The structure that implements a 20 mm gap has a stiffness of 0.26 times than in a gapless of FDG. The hysterical curve of the friction damper without a gap compared to the others applying the 20 mm of gap is shown in each of **Fig. 12**.

At the deformation limit, structures with FDG are capable of generating significant dissipation energy. While the column group structure with no friction device and with rigid friction device equally pro-

duce the dissipated energy close to zero as in **Fig. 11**. The dissipated energy quantity of each structural variation is presented in **Table 5**. The maximum of dissipated energy occurs in each steel reinforcement ratio and the same gap length group at certain fractional values of the friction damper. Appropriate FDG confinement force values must be determined to achieve optimal dissipated energy capacity. The dissipated energy optimization in the variation of FDG confinement force and the number of cross-section bars shown in **Fig. 9**, the greater the proportion of reinforced steel cross-section the greater the energy dissipation produced. While the relation of the gap length to the dissipated energy is shown in **Fig. 10**. Based on **Fig. 10**, the longer the gap is applied, the smaller the dissipation energy will be achieved. The structural variation num-

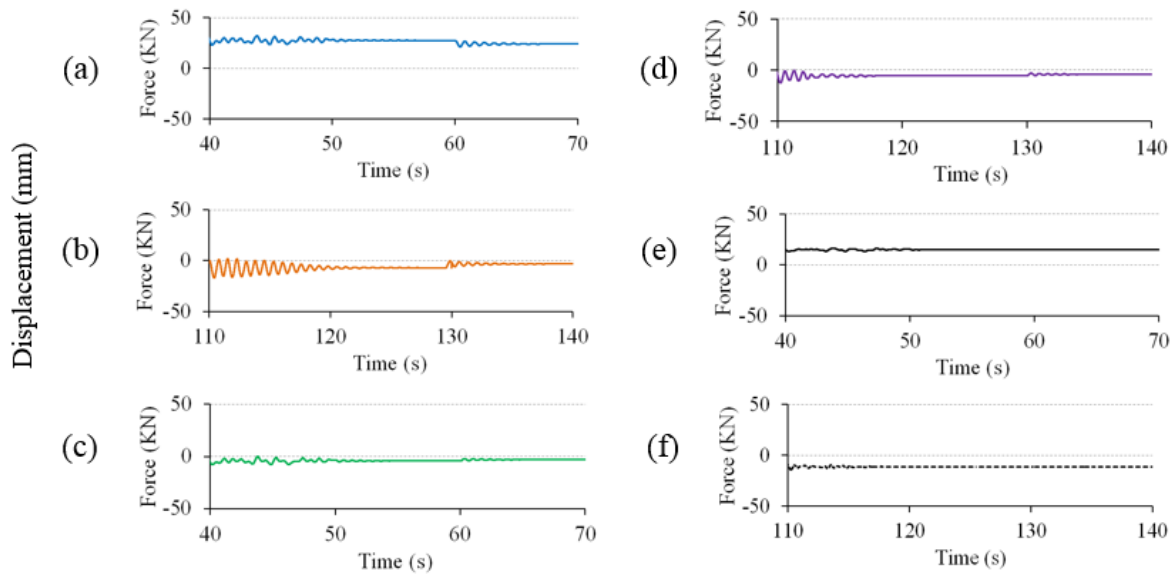


**Fig. 15** The maximum residual displacement response of the structure under seismic load level 2; (a) Str3, (b) Str9, (c) Str15, (d) Str21, (e) Str25, and (f) Str26.

ber 19 configured with 1.62% reinforcing steel and 10200 kN strength force that has the largest dissipated energy capacity in the scenario is chosen for the structural performance examination. The ratio of the equivalent damping ratio ( $\eta$ ) of it is 23%, as shown in **Table 5**. The proposed structure which implements the 20 mm gap target achieves a damping ratio of 18%.

Structure with scenario 1 has a deformation limit capacity (in drift ratio) of 0.7%, structure with scenario 2 of 1.3%, and structures with scenarios 3 and 4 have a deformation capacity limit of 1.4% of drift ratio. The use of high-grade material (USD685) of reinforcement in the middle column can significantly increase the deformation limit capacity. While the use of this in the middle and edge of the column is almost the same as its use in the middle column only. The use of high-grade steel materials also significantly increases structural strength both in the occurrence of FDG post-slip and at deformation limit. This reason will be explained in the next paragraph below. The structural behavior in the entirety of deformation limit capacity and structural strength can be observed in **Fig. 11**.

The use of reinforcement with high-strength steel (USD685) material will increase the dissipated energy. This is due to increased deformation limit capacity as well as increased structural strength. The implementation of high-grade reinforcing steel in the middle column and ordinary-grade reinforcing steel in the side column with is significant enough to achieve large dissipated energy.

Although the dissipated energy of this structure (Scnr2) is slightly smaller than that implements all reinforcing bars using high-grade steel (Scnr3 and Scnr4), it makes prosper in terms of the construction cost. While the damping ratio of the structures with Scnr2, Scnr3, dan Scnr4 are similar; this statement is supported by the data in **Table 5** and **Fig. 11**.

The determination of deformation limit based on yielding stress of reinforcing steel in different column positions will result in nearly equal deformation capacity but different strength. The limit state of scenario 4 (Scnr4) is more stringent than scenario 3 (Scnr3). In the scenario 4 the structure is expected to behave fully elastic. Envisaged in scenario 3, the structure still occurring plastic deformation on the side column. The result of the dissipated energy scenario three will require a larger FDG confinement force than the scenario four. The larger the FDG confinement force, the larger the structural strength, but the elastic limit of the deformation capacity of the center column is almost identical, illustrated in **Fig. 13**. Comparison the energy dissipation scenario 3 and scenario 4 of the structure are shown in **Table 5**.

## (2) Structural performance

The structural performance target that remains elastic under Level 2 of earthquake excitation can be achieved in several structural variations. All structures with scenario 1 (Scnr1) are not capable of achieving performance target, the structure with

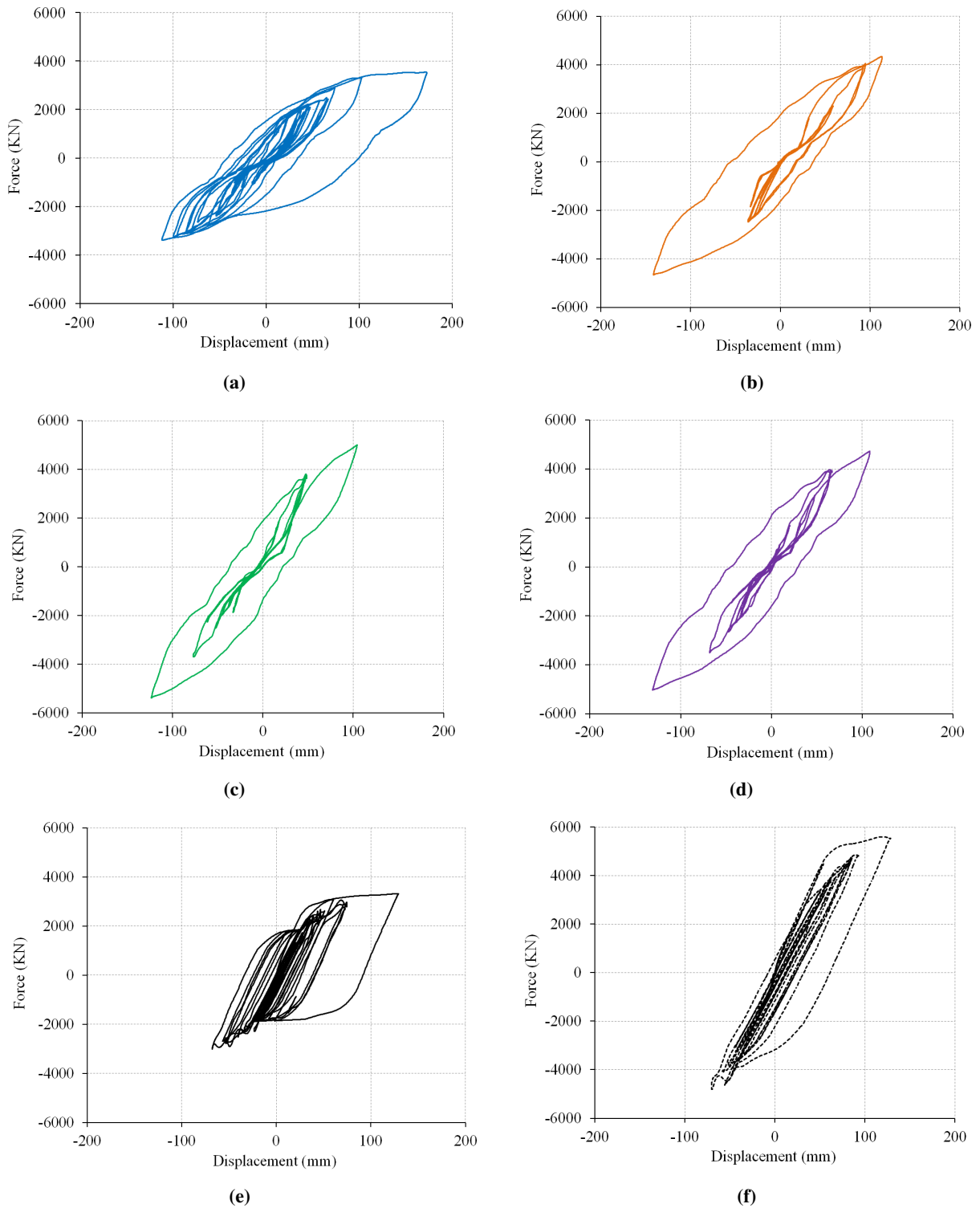


**Fig. 16** The force and displacement seismic response of; (a) Str3, (b) Str9, (c) Str15, (d) Str21, (e) Str25, and (f) Str26.

scenario 2 (Scnr2) is deformed below the deformation limit in the application of a 10 mm gap, and the structures with scenario 3 and 4 are capable of achieving the performance target with 20 mm gaps, as in **Table 4**. On earthquake excitation, the proposed structure's hysteretic curve corresponds to the structural hysteretic curve at the static loading, as in **Fig. 14**.

The proposed structure (with 20 mm gap) of Str15 and Str21 is capable of behaving elastically under Level 2 of earthquake excitation with a maximum displacement near to the conventional structure of **Fig. 14**. While the column reinforcement that implement combination with ordinary-grade and high-grade (Str9) in the scenario 2 exceeded from its deformation limit with a deformation ratio of 1.05.

The maximum response and the limit state of the structure are described in **Fig. 13f** and **Table 5**. The application of high strength steel reinforcement is required to achieve sufficient dissipated energy and deformation limit of the structure with elastic behavior (Performance 1). The force and deformation relation of the maximum response under seismic excitation of the structure are shown on **Fig. 16**.

The proposed structures in scenes 2, 3, and 4 produce smaller residual deformations than conventional pier structures as shown on **Fig. 15**. This happens because, in scenario 2 and 3, the middle structure is remains elastic behavior, while in scenario four all structure columns still experience the elastic behavior. Structure approaching elastic behavior will have a good recentering ability.

## 6. CONCLUSIONS

The integrated bridge pier with triple RC column accompanied by friction damper plus gap is successfully proposed to accommodate a 20 mm length of thermal expansion slot. This structure can behave elastic or near elastic conditions under severe earthquake excitation. The elastic behavior of the structure also manifests small residual deformations. Based on the analysis, the structure has the following behaviors and performance:

- (a) The gap length, the proportional cross-sectional area of the reinforcing steel, and friction damper strength shall be determined proportionately to achieve the high seismic performance structure. The longer of the gap, the smaller of the dissipated energy produced. The greater the reinforcing steel proportion, the greater the strength and the dissipated energy. While the friction force value need to be determined at the optimum dissipated energy.
- (b) In the optimum dissipated energy, the implementation of different location limits will affect the strength and the dissipated energy of the structure significantly. While deformation limit capacity is not affected significant.
- (c) The use of high strength steel reinforcement in the central column will increase the deformation limit capacity, strength, and dissipated energy. While the application of high strength steel reinforcement for all columns is slightly better in improving the performance of the structure than the application that is only in the middle of the column.
- (d) The application of the 20 mm gap in the FDG

resulted in the stiffness of the structure 0.26 times smaller than without the gap.

- (e) The structure without and with gap can achieve an equivalent damping ratio 22%-23% and 18% respectively.
- (f) Str15 and Str21 are still below the elastic limit under Level 2 of seismic excitation, while all conventional columns have undergone plastic conditions.
- (g) The maximum response of the Str9 slightly exceed the limit state. It has potential to be improved and to be implemented for the real structure because it is more economical than the Str15 and Str21.
- (h) The residual deformation of Str9, Str15, and Str21 are significantly smaller than that of the conventional column structures.

## Acknowledgements

This research was partially supported by JSPS Grant-in-Aid for Scientific Research(B) Grant Number JP26289145. The authors would also like to thank Prof. Sumio Sawada, Disaster Prevention Research Institute, Kyoto University for the fruitful discussion.

## References

- 1) F.C. Filippou: FEDEAS - Finite Elements for Design, Evaluation, and Analysis of Structures Theory, Reference Manual and Example, Technical report, Department of Civil Engineering, University of California, California, 1996.
- 2) FEMA: *Prestandard and Commentary for the Seismic Rehabilitation of Buildings*, 1, Federal Emergency Management Agency, Washington, D.C., 2000.
- 3) Filippou, F.C. and Issa, A.: Nonlinear Analysis of Reinforced Concrete Frames under Cyclic Load Reversals, Technical Report December, Earthquake Engineering Research Center College of Engineering University of California, Berkeley, California, 1988.
- 4) Filippou, F.C., Popov, E. and Bertero, V.: Effects of Bond Deterioration on Hysteretic Behavior of Reinforce Concrete Joint, Technical Report August, Earthquake Engineering Research Center, California, 1983.
- 5) Iemura, H., Takahashi, Y. and Sogabe, N.: Two-level seismic design method using post-yield stiffness and its application to unbonded bar reinforced concrete piers, *Structural Engineering/Earthquake Engineering*, volume 23, no. 1:109–116, 2006.
- 6) Japan Road Association: *Specifications for Highway Bridges: Part V Seismic Design*, Maruzen Co. Ltd., Tokyo, 2012.

- 7) Mazzoni, S., McKenna, F., Scott, M.H. and Fenves, G.L.: *OpenSees Command Language Manual*, 2007.
- 8) Menegotto, G., Pinto, M. and Emilio, P.: Method of Analysis for Cyclically Loaded R.C. Plane Frames Including Changes in Geometry and Non-Elastic Behavior of Elements under Combined Normal Force and Bending, in *Proceedings of IABSE Symposium on Resistance and Ultimate Deformability of Structures Acted on by Well Defined Loads*, pages 15–22, Zurich, 1973.
- 9) Mualla, I. and Belev, B.: Performance of Steel Frames with a New Friction Damper Device under Earthquake Excitation, *Engineering Structures*, volume 24, no. 3:365–371, 2002.
- 10) Nakamura, H., Takahashi, Y. and Sawada, S.: *The Elasto-Plastic Behavior of the Rectangular RC Column Accompanied with Friction Damping Mechanism with Complex Confinement*, Undergraduate thesis, Kyoto University, 2011.
- 11) Nakamura, H., Takahashi, Y. and Sawada, S.: The Elasto-plastic Behavior of the Rectangular RC Column Accompanied with Friction Damping Mechanism, volume 68, no. 4:577–583, 2012.
- 12) Nakamura, H., Takahashi, Y. and Sawada, S.: *The Study on Earthquake Response Mechanism of Set RC Columns with Unity of Frictional Damping Mechanism*, Ph.D. thesis, Kyoto University, 2013.
- 13) Neuenhofer, A. and Filippou, F.C.: Evaluation of Nonlinear Frame Finite-Element Models, *Journal of Structural Engineering*, volume 123, no. May:583–590, 1997.
- 14) Pall, A.: *Limited Slip Bolted Joints : a Device to Control the Seismic Response of Large Panel Structures*, Doctoral thesis, Concordia University, 1979.
- 15) Pall, A., Marsh, C. and Fazio, P.: Friction Joints for Seismic Control of Large Panel Structures, *PCI Journal*, volume 25, no. 6:38–61, 1980.
- 16) Pall, A.S. and Marsh, C.: Response of Friction Damped Braced Frames, volume 108, no. June:1313–1323, 1982.
- 17) Ramirez, J.D.M. and Tirca, L.: Numerical Simulation and Design of Friction- Damped Steel Frame Structures damped, in *15th World Conference in Earthquake Engineering*, Lisboa, 2012.
- 18) Scott, M.H. and Hamutçuoğlu, O.M.: Numerically Consistent Regularization of Force-based Frame Elements, *International Journal for Numerical Methods in Engineering*, volume 76, no. 10:1612–1631, 2008.
- 19) Setiawan, A.F., Takahashi, Y., Kiyono, J. and Sawada, S.: Numerical Analysis of RC Columns Accompanied with Friction Damping Mechanism under Cyclic Loading, in *Procedia Engineering*, volume 171, pages 821–835, Denpasar, 2017.
- 20) Spacone, E.: Fibre Beam-Column Model for Non-Linear Analysis of R/C Frames : Part II. Applications, volume 25, no. January:727–742, 1996.
- 21) Taucer, F.F. and Spacone, E.: Aa Fiber Beam-Column Element for Seismic Response Analysis of Reinforced Concrete Structures, Technical Report December 2014, Earthquake Engineering Research Center College of Engineering University of California, Berkeley, California, 1991.